



PERGAMON

Available online at [www.sciencedirect.com](http://www.sciencedirect.com)

SCIENCE @ DIRECT®

Radiation Physics and Chemistry 68 (2003) 351–356

Radiation Physics  
and  
Chemistry[www.elsevier.com/locate/radphyschem](http://www.elsevier.com/locate/radphyschem)

# Characterization of nanoporous ultra low- $k$ thin films templated by copolymers with different architectures

Shu Yang<sup>a,\*</sup>, Peter Mirau<sup>a</sup>, Jianing Sun<sup>b</sup>, David W. Gidley<sup>b</sup><sup>a</sup> Bell Labs, Lucent Technologies, 600 Mountain Ave., Murray Hill, NJ 07974, USA<sup>b</sup> Department of Physics, University of Michigan, Ann Arbor, MI 48109, USA

## Abstract

Triblock, diblock and random copolymers of poly(ethylene oxide) and poly(propylene oxide) are used as molecular templates in poly(methyl silsesquioxane) (MSQ) matrices to fabricate ultra low- $k$  dielectric materials ( $k \leq 2.0$ ). Solid-state NMR shows that polymer architecture plays an important role in the polymer domain size and the polymer–matrix interface in the nanocomposites. Positronium annihilation lifetime spectroscopy reveals that porous MSQ film templated by triblock copolymers ( $\bar{M}_n$  in the range of  $\sim 5000$ – $12,000$  g/mol) have smallest pores and highest percolation threshold compared to those templated by diblock and random copolymers.

© 2003 Elsevier Science Ltd. All rights reserved.

## 1. Introduction

In the semiconductor industry, device features in integrated circuits (IC) continue to shrink to increase microprocessor speed and the density of devices packed on circuits. When the packing density between multilevel interconnects increases, current dielectric material, silicon dioxide, which has a dielectric constant ( $k$ ) of  $\sim 4.0$ , will no longer be adequate for next generation ICs. Therefore, a new low dielectric constant material needs to be identified to minimize RC delay according to Semiconductor Industry Association (2001). By taking advantage of the low dielectric constant of air,  $k = 1$ , dielectric constant can be successfully decreased to less than 2 with more than 30–50% porosity in the thin film as shown by Ramos (1997), Jin et al., (1998), Nguyen (1999), Bremmer (1997).

Although different materials have been tested as the matrix, an organic/inorganic hybrid silicate, methyl silsesquioxane (MSQ) has been chosen as one of the leading candidates as on-chip low- $k$  materials due to its intrinsically low dielectric constant ( $k \sim 2.6$ – $2.8$ ) and its hydrophobic nature. It maintains good mechanical and thermal stability close to inorganic oxide, yet has lower dielectric constant due to the presence of microporosity

and lower density. Only 30% porosity is required to reach  $k \leq 2.0$ . Based on MSQ matrix, different sacrificial templates have been studied by Nguyen (1999, 2000) and Yang et al. (2002) as porogens to generate pores, ideally less than 10 nm. Previously, we have reported using amphiphilic triblock copolymers, poly(ethylene oxide-*b*-propylene oxide-*b*-ethylene oxide) (PEO-*b*-PPO-*b*-PEO) as porogens in MSQ to attain ultra low-dielectric constants ( $k \approx 1.5$ ) with good electrical and mechanical properties (Yang, 2002). The microphase separation of triblock copolymers plays an important role to prevent macroscopic aggregation in MSQ and the properties of porous materials can be controlled at the molecular level. Extremely small pores (2–6 nm) are generated. To further understand the correlation between the phase separation, interaction length scale, pore structure and molecular weight, architecture of the templating materials, we compare porous films templated by triblock, diblock and random copolymers of poly(ethylene oxide) (PEO) and poly(propylene oxide) (PPO). Solid-state <sup>1</sup>H NMR shows that although all copolymers templates microphase separate from MSQ matrix, the interaction between copolymer and MSQ depends significantly on the polymer architecture. In the nanocomposites templated by triblock copolymers, the hydrophobic PPO blocks stay at the interface; in those templated by diblock copolymers, PPO blocks dissolve in the MSQ matrix; in the case of random copolymers, both PEO

\*Corresponding author. Fax: +1-908-582-4868.

E-mail address: [syang6@lucent.com](mailto:syang6@lucent.com) (S. Yang).

and PPO are found at the interface while PEO is more dominant. The structures of the nanocomposites define the final pore structures in the thin film, which determines the film electrical and mechanical properties. We investigate the relationship between pore structure (pore size and percolation threshold) and polymer architecture by positronium annihilation lifetime spectroscopy (PALS).

## 2. Experimental section

### 2.1. Materials

Triblock copolymers of poly(ethylene oxide-*b*-propylene oxide-*b*-ethylene oxide) (PEO-*b*-PPO-*b*-PEO), Pluronic<sup>®</sup> F88 (80 wt% PEO,  $\bar{M}_n$  of 11,250 g/mol), P103 (30 wt% PEO,  $\bar{M}_n$  of 4950 g/mol), F38 (80 wt% PEO,  $\bar{M}_n$  of 4700 g/mol) and P105 (50 wt% PEO,  $\bar{M}_n$  of 6500 g/mol) were obtained from BASF. The diblock copolymer ( $\bar{M}_n$  of 5500 and 1100 g/mol for the PEO and PPO blocks, respectively) was obtained from Polymer Source, Inc. The random copolymer (75 wt% PEO,  $\bar{M}_n$  of 12,000 g/mol) was obtained from Aldrich. The films were prepared in the same way described in the literature Yang et al. (2002).

### 2.2. Characterization

The solid-state proton NMR experiments were performed at 400 MHz using a Varian Unity NMR spectrometer with a 4 mm magic-angle spinning probe and spinning speed regulation at 12 kHz. The proton pulse widths were 3.5  $\mu$ s and the dipolar filter pulse sequence (Egger, 1992) was used to measure the chain dynamics and for the spin diffusion experiments. PALS spectra with  $10^7$  events were acquired at room temperature with a conventional fast–fast lifetime system with a resolution of 500 ps. POSFIT program was used for data fitting and the Ps lifetime can be correlated with pore size using the extended Tao-Eldrup model (Dull et al., 2001). The uncapped samples were studied at two implantation energies, 5.0 and 1.0 keV, to search for any depth related heterogeneity. When open porosity of the films was detected, an 80 nm silica cap was deposited to confine Ps to the pores in the film.

## 3. Results and discussion

Block copolymers have unique amphiphilic characteristics that they tend to microphase separate into different domains (Bates and Fredrickson, 1990). For example, PEO-*b*-PPO-*b*-PEO triblock copolymers have been extensively studied as polymeric surfactants and self-assembled systems (Alexandridis et al., 1994; Yang,

1998; Schmolka, 1977). Compared to diblock copolymers, triblock copolymers are entropically less favored to form a large micelle since the junction between two blocks per molecule is restricted to reside in the core–shell interface (Hamley, 1998). This means smaller polymer domain may form in the triblock copolymer templated nanocomposite. For random copolymers, the lack of specific interaction between polymer and matrix means less restriction for a larger association number. A larger polymer domain and early percolation may be expected. Here, we use the copolymers of PEO and PPO with different polymer architectures as sacrificial templates to generate porous MSQ films.

### 3.1. Polymer microstructure in nanocomposites

The microstructure of polymer in MSQ and the polymer–MSQ interaction determine the final pore size and structure. Since the glass transition temperatures for PEO and PPO ( $\approx -70^\circ\text{C}$ ) are well below the ambient temperature, it is possible to use solid-state proton NMR with fast magic angle spinning (MAS) to study the structure and dynamics in our nanocomposites. The thin films were prepared by spin coating on Si wafers, followed by heating at  $120^\circ\text{C}$  for 12 h. Then the films were scratched off for solid-state NMR study. In the triblock (F88)/MSQ composites, the cross section through the CH/CH<sub>2</sub> peak from 2D exchange NMR shows mainly diagonal peak intensity with little spin diffusion to peaks at 1 and 0 ppm, suggesting little interaction between PEO and MSQ matrix (see Fig. 1a). Cross sections through the PPO CH<sub>3</sub> peak (Fig. 1b) show large cross peaks to both the CH/CH<sub>2</sub> peak and the MSQ CH<sub>3</sub> peak, indicating that PPO and MSQ must be in close proximity. A core–shell structure in MSQ is proposed that the more hydrophobic PPO block is next to the hydrophobic MSQ, while the hydrophilic PEO is buried inside (Yang, 2001). Formation of such structure facilitates miscibility between the triblock copolymers and the MSQ, and polymers are microphase separated in nanometer length scale.

Similarly, diblock copolymers form a core–shell structure in MSQ. However, a larger cross section peak between PPO and MSQ methyl groups is observed (see Fig. 2b), indicating a closer distance between them since the rate of magnetization exchange depends on the inverse sixth power of the internuclear distance and on the chain dynamics. In comparison, the relative intensity of the CH/CH<sub>2</sub> diagonal peak in the random/MSQ composites is the smallest, showing that the exchange with other peaks is most efficient (see Fig. 3a). For the magnetization that is exchanged, the intensity of the MSQ peak and PPO methyl peaks are nearly equal. The PPO methyl peak shows efficient exchange both to the matrix and the CH/CH<sub>2</sub> peak (see Fig. 3b). This suggests that PEO and PPO chains are not strongly

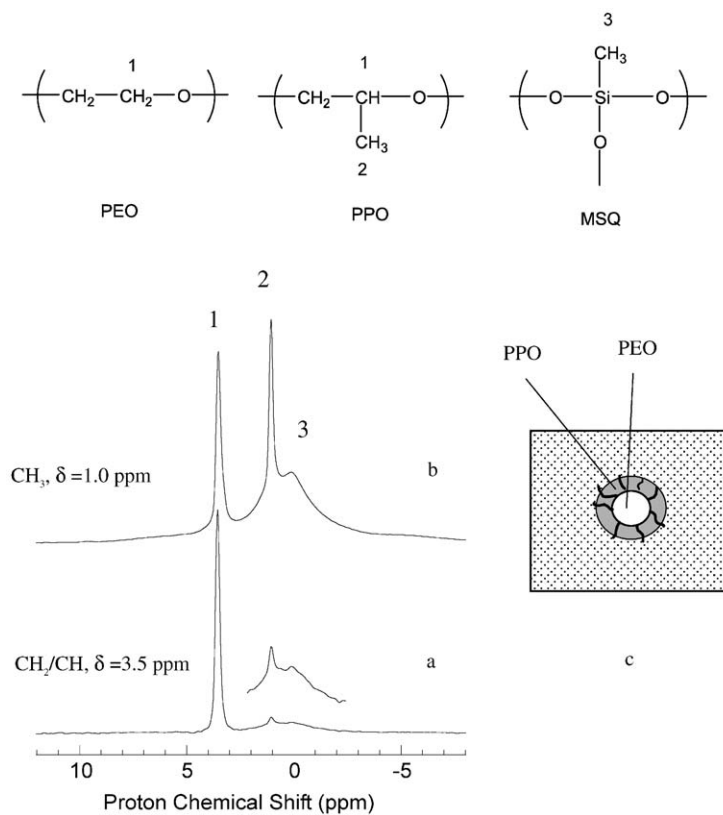


Fig. 1. Cross sections through the 2D exchange  $^1\text{H}$  NMR spectrum for the F88/MSQ composite at the chemical shift of (a) 3.5 and (b) 1.0 ppm. **1.** CH and  $\text{CH}_2$  groups in the polymer backbone; **2.**  $\text{CH}_3$  groups in PPO; **3.**  $\text{CH}_3$  groups in MSQ. (c) Schematic structure of phase behavior of PEO-*b*-PPO-*b*-PEO triblock copolymers in MSQ thin film cured at  $120^\circ\text{C}$  for 12 h.

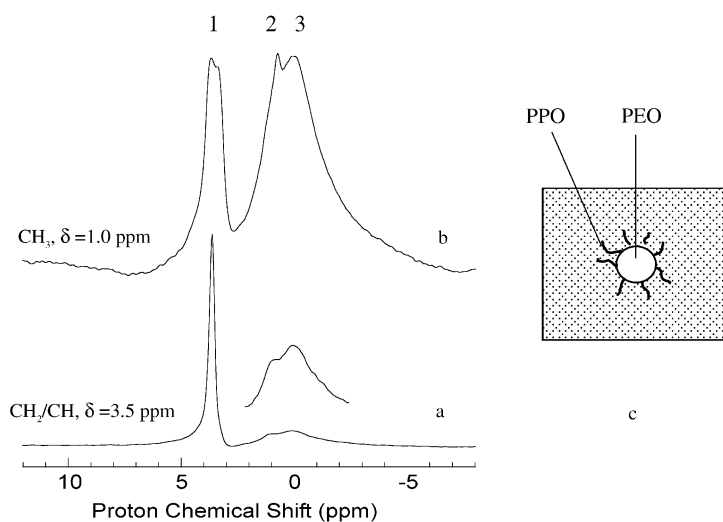


Fig. 2. Cross sections through the 2D exchange  $^1\text{H}$  NMR spectrum for the Diblock/MSQ composite at the chemical shift of (a) 3.5 and (b) 1.0 ppm. **1.** CH and  $\text{CH}_2$  groups in the polymer backbone; **2.**  $\text{CH}_3$  groups in PPO; **3.**  $\text{CH}_3$  groups in MSQ. (c) Schematic structure of phase behavior of PEO-*b*-PPO diblock copolymers in MSQ thin film cured at  $120^\circ\text{C}$  for 12 h.

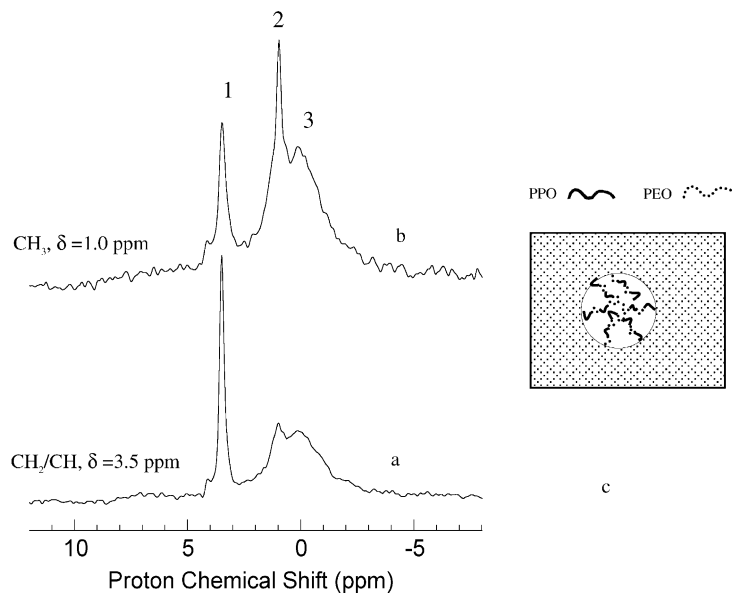


Fig. 3. Cross sections through the 2D exchange <sup>1</sup>H NMR spectrum for the Random/MSQ composite at the chemical shift of (a) 3.5 and (b) 1.0 ppm. **1.** CH and CH<sub>2</sub> groups in the polymer backbone; **2.** CH<sub>3</sub> groups in PPO; **3.** CH<sub>3</sub> groups in MSQ. (c) Schematic structure of phase behavior of PEO-*r*-PPO random copolymers in MSQ thin film cured at 120°C for 12 h.

microphase separated as those in block copolymers. Although PPO is still dominant at the polymer–matrix interface, some PEO chains are present as well.

A further study by Mirau and Yang (2002) using dipolar filter pulse sequence shows that copolymers architectures have a fundamentally different effect on the polymer chain dynamics in the composites. In F88/MSQ, the polymer peaks are partially reduced by the dipolar filter, but the relative peak intensities are similar to those in the equilibrium spectrum. This means that both the PEO and PPO blocks are mobile and not strongly attenuated by the dipolar filter. A three-phase model with PPO at interface is suitable for triblock/MSQ composite (see Fig. 1c). In diblock/MSQ, PPO methyl peak is strongly attenuated when the filter strength is increased, suggesting that the PPO blocks are restricted and dissolved in the matrix (see Fig. 2c). In these block copolymer templated nanocomposites, the formation of a core–shell structure makes it possible the self-assemble block polymers into small and isolated domains, which may result in small and closed pores. In comparison, in the random copolymer composite the dipolar filter has only a small effect on the polymer peaks, but efficiently suppressed the MSQ signal at 0 ppm. A two-phase model that does not have strong phase separation is proposed for random/MSQ (see Fig. 3c). It may result in larger aggregation of polymer chains and their early percolation.

After heating the composites to above 400°C, polymers are decomposed and pores are generated. Small (less than 10 nm) and closed pores are preferred since

large and open pores make the thin film more susceptible to metal diffusion that could adversely affect the electrical or mechanical properties, as well as the adhesion to the interface. A technique that can quantitatively characterize pore structures, such as pore size, distribution, interconnectivity, and porosity in sub-micron film on-chip is needed. Compared to traditional techniques, such as N<sub>2</sub> absorption and transmission electron microscopy (TEM), techniques such as ellipsometry (Postava and Yamaguchi, 2001), combination of X-ray reflectivity and small angle neutron scattering (XR/SANS) (Wu, 2000), and positronium annihilation lifetime spectroscopy (PALS) (Gidley et al., 2000) can non-destructively measure the nanometer-sized pore structure of thin film as processed on the silicon wafer. PALS is of particular interest to us since it is highly sensitive to void size as small as several Å and can be used to probe closed pores (Gidley et al., 2000).

In PALS experiment, a focused beam of several keV positrons is generated in a high vacuum system. When it is hit on the sample film, positronium (Ps, the electron–positron bound state) is formed and tends to localize in open-volume pores. If the pore is closed, Ps natural annihilation lifetime of 142 ns is then reduced by annihilation with molecular electrons during collisions with the pore surface. The reduced Ps annihilation lifetime is associated with the average pore size as measured by its mean free path. If the pores are interconnected, the highly mobile Ps can readily diffuse out of the film and escape into the vacuum, resulting a lifetime same as the vacuum lifetime, 142 ns. When

interconnected pores are detected, an 80 nm silica cap is deposited to confine Ps to the pores in the film. Thus, only one average mean free path of Ps throughout the film is obtained, which corresponds to a single lifetime component in PALS measurement. Comparison of Ps intensities in the film and in the vacuum will allow us to determine the evolution of pore structures and the threshold for pore percolation along with the loading of polymer templates.

### 3.2. Pore interconnectivity and percolation threshold

The intensity of Ps annihilating in the film (including Ps in both mesopores and micropores) comes from Ps annihilating in the closed porosity, while those in the vacuum is from backscattering ( $\sim 2\%$  at 5.0 keV) and escaping from open porosity. As shown in Fig. 4, when the loading of triblock copolymers, F88, is less than 20 wt%, the vacuum Ps intensity is consistent with backscattered Ps, indicating that there are mainly closed pores. The amount of Ps that annihilates in the film stays relatively stable until a sudden drop occurs when the loading of F88 increases to 25 wt%. At the same time, Ps intensity in vacuum increases significantly. This trend continues until F88 loading reaches 40 wt% and then both intensities level off. Therefore, 20 wt% loading is considered as the nominal pore percolation threshold, above which the pores merge with surrounding pores and form open paths to the free surface. The diffusion of Ps is still frustrated by the pore morphology at 25 wt% loading since some Ps still annihilates in the film. As the loading of F88 increases above 40 wt%, the porous network is totally interconnected because nearly all the Ps in the mesopores escape into vacuum. In contrast, the percolation threshold in the random copolymer

templated films occurs in the range of 10–20 wt% loading, much lower than that in the triblock templated films ( $\sim 20$  wt%) (see Fig. 4). In the series of diblock copolymer templated films, while closed pores are observed at 15 wt% loading, they become interconnected at 25 wt% loading and are completely interconnected at 30 wt% loading. It is not clear whether the percolation threshold is 15 or 20 wt% due to the low Ps signal at 20 wt%, and more work is underway. The microporosity generated by removing PPO, which is dissolved in MSQ, may contribute to the frustration of Ps at the percolation threshold.

### 3.3. Determination of pore sizes

Closed micropores ( $\sim 0.6$ – $1.1$  nm) are detected in all films and appear to be characteristic of the MSQ matrix. Below percolation threshold, closed pores are present mainly in the porous films. In the F88/MSQ films, an intermediate Ps lifetime, 28 and 33 ns, respectively, is observed in the film at the loading of 15 and 20 wt%, respectively. When the F88 loading goes beyond the percolation threshold ( $\sim 20$  wt%), a capping layer (80 nm silica) is used as Ps diffusion barrier to measure the intrinsic pore size in interconnected porous network. For interconnected pores, a two-dimensional tubular pore model is used, while for isolated pores a three-dimensional cubic pore model is used for fitting. As seen in Fig. 5, the pore size increases with the loading of F88. A pore size of  $2.7 \pm 0.2$  nm is obtained in the film with 30 wt% F88 loading. Similarly, we have measured the pore size in other triblock copolymer templated porous MSQ. For example, in the films with 30 wt% of P103, F38 and P105, respectively, the pore sizes are  $3.5 \pm 0.2$ ,  $3.5 \pm 0.2$  and  $3.4 \pm 0.2$  nm, respectively. When the F88 loading increases to 50 wt%, the pore sizes remain small,  $4.8 \pm 0.3$  nm, while the dielectric constant decreases to 1.5. In porous films templated from random copolymers, an intermediate lifetime of 24 ns is found at 10 wt% loading, which corresponds to a closed pore with diameter of 1.4 nm. When the loading increases to 20 wt%, pores are interconnected with an average pore size of  $5.6 \pm 0.3$  nm compared to closed pores ( $2.2 \pm 0.2$  nm) in F88/MSQ films. In diblock templated films, the pore sizes are  $2.3 \pm 0.1$  and  $3.8 \pm 0.2$  nm, corresponding to 15 and 30 wt% loading, respectively. The sizes are slightly larger than those templated by triblock copolymers.

Clearly, the architecture of the polymer template has a significant influence on the final porous size, pore structure and its percolation threshold. It is consistent to the microstructures of nanocomposites studied by the solid-state NMR. The formation of a core-shell structure by block copolymers in the nanocomposite results in smaller pores and higher percolation threshold compared to random copolymer templated films;

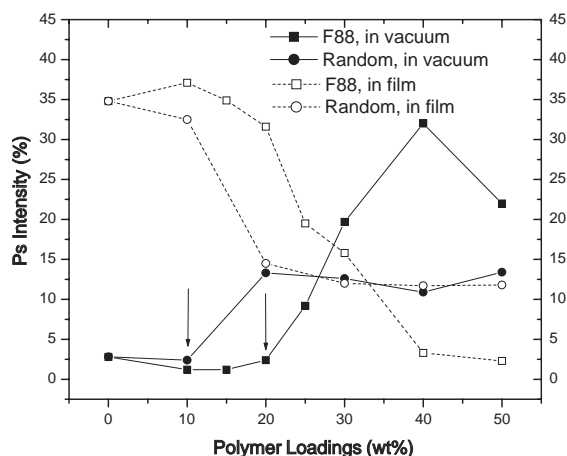


Fig. 4. Ps in-film intensities and vacuum intensities in the porous MSQ films as a function of polymer loadings. The arrows point to the percolation threshold for each series. Data acquired with deep positron implantation at 5 keV energy.

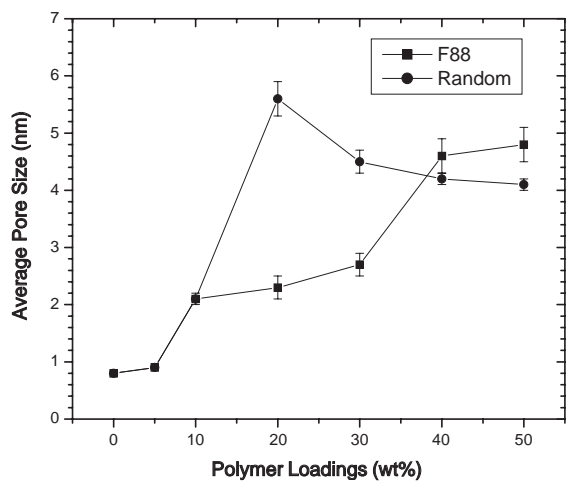


Fig. 5. Comparison of average pore sizes in porous MSQ films templated by triblock and random copolymers.

triblock copolymers are entropically less favored to form a larger domains/pores compared to diblock, thus, generate the smallest pores.

#### 4. Conclusions

Triblock, diblock and random copolymers of poly(ethylene oxide) (PEO) and poly(propylene oxide) (PPO) act as molecular templates in poly(methyl silsesquioxane) (MSQ) matrices to fabricate ultra low- $k$  materials ( $k \leq 2.0$ ). Solid-state NMR and PALS have been used to study the structures of nanocomposites and nanopores, respectively. It is found that the polymer architecture plays an important role to the polymer–matrix interaction and the final pore size and percolation threshold. In the system we studied that polymer's average number molecular weight ( $\bar{M}_n$ ) ranges from  $\sim 5000$  to  $12,000$  g/mol, porous MSQ films templated by triblock copolymers have the smallest pores and highest percolation threshold compared to those templated by diblock and random copolymers.

#### Acknowledgements

We would like to thank E. Reichmanis and O. Nalamasu for helpful discussion. We acknowledge the support from National Science Foundation (NSF) through grant ECS-9732804 with UM.

#### References

Alexandridis, P., Holzwarth, J.F., Hatton, T.A., 1994. Micellization of poly(ethylene oxide)–poly(propylene oxide)–poly

(ethylene oxide) triblock copolymers in aqueous-solutions-thermodynamics of copolymer association. *Macromolecules* 27, 2414–2425.

- Bates, F.S., Fredrickson, G.H., 1990. Block copolymer thermodynamics: theory and experiment. *Annu. Rev. Phys. Chem.* 41, 525–557.
- Bremmer, J.N., et al., 1997. Cure of hydrogen silsesquioxane for intermetal dielectric applications. In: Case, C., Kohl, P., Kikkawa, T., Lee, W.W. (Eds.), *Low-dielectric Constant Materials*, Vol. III. Mater. Res. Soc., Pittsburgh, pp. 37–44.
- Dull, T.L., et al., 2001. Determination of pore size in mesoporous thin films from the annihilation lifetime of positronium. *J. Phys. Chem. B* 105, 4657–4662.
- Egger, N., et al., 1992. Solid-state NMR investigation of cationic polymerized epoxy-resins. *J. Appl. Polym. Sci.* 44, 289–295.
- Gidley, D.W., et al., 2000. Determination of pore size distribution in low dielectric thin films. *Appl. Phys. Lett.* 76, 1282–1284.
- Hamley, I.W., 1998. *The Physics of Block Copolymers*. Oxford University Press, Oxford.
- Jin, C., List, S., Zielinski, E., 1998. Porous silica xerogel processing and integration for ULSI applications. In: Chiang, C., Ho, P.S., Lu, T.-M., Wetzel, J.T. (Eds.), *Low-dielectric Constant Materials*, Vol. IV. Mater. Res. Soc., Warrendale, pp. 213.
- Mirau, P.A., Yang, S., 2002. Solid-state proton NMR characterization of ethylene oxide and propylene oxide random and block copolymer composites with poly(methyl silsesquioxanes). *Chem. Mater.* 14, 249–255.
- Nguyen, C.V., et al., 1999. Low-dielectric, nanoporous organosilicate films prepared via inorganic/organic polymer hybrid templates. *Chem. Mater.* 11, 3080–3085.
- Nguyen, C.V., et al., 2000. Hyperbranched polyesters as nanoporosity templating agents for organosilicates. *Macromolecules* 33, 4281–4284.
- Postava, K., Yamaguchi, T., 2001. Optical functions of low- $k$  materials for interlayer dielectrics. *J. Appl. Phys.* 89, 2189–2193.
- Ramos, T., et al., 1997. Nanoporous silica for low- $k$  dielectrics. In: Lagendijk, A., Treichel, H., Uram, K.J., Jones, A.C., (Eds.), *Low-dielectric Constant Materials*, II, Vol. 443. Mater. Res. Soc., Pittsburgh, PA, pp 91–98.
- Schmolka, I.R., 1977. *J. Am. Oil Chem. Soc.* 54, 110.
- Semiconductor Industry Association, 2001. *International Technology Roadmaps of Semiconductors*.
- Yang, P.D., et al., 1998. Triblock-copolymer-directed syntheses of large-pore mesoporous silica fibers. *Chem. Mater.* 10, 2033–2036.
- Yang, S., et al., 2001. Molecular templating of nanoporous ultralow dielectric constant (approximate to 1.5) organosilicates by tailoring the microphase separation of triblock copolymers. *Chem. Mater.* 13, 2762–2764.
- Yang, S., et al., 2002. Nanoporous ultralow dielectric constant organosilicates templated by triblock copolymers. *Chem. Mater.* 14, 369–374.
- Wu, W.L., et al., 2000. Properties of nanoporous silica thin films determined by high-resolution X-ray reflectivity and small-angle neutron scattering. *J. Appl. Phys.* 87, 1193–1200.